Search for di-Higgs production with the ATLAS detector

Wiliam Davey[*] **on behalf of the ATLAS Collaboration**
University of Bonn (DE)
E-mail: will.davey@cern.ch

A search for resonant and non-resonant di-Higgs production in the *bbbb*, $\gamma\gamma bb$ and $\gamma\gamma WW^*$ channels is presented. The analysis uses 3.2–13.3 fb^{-1} of proton–proton collision data at $\sqrt{s} = 13$ TeV collected by the ATLAS detector at the Large Hadron Collider (LHC). No excess is observed and upper limits are placed on the di-Higgs production rate in the Standard Model (SM) and in various beyond SM scenarios. Future prospects for the observation of non-resonant SM di-Higgs production with the high-luminosity LHC are also presented.

---

[*]Speaker.

1. Introduction

The discovery of a Higgs boson (h) at the Large Hadron Collider (LHC) motivates searches for Higgs boson pair production (di-Higgs production). Di-Higgs production in the Standard Model (SM) proceeds at leading order via a box-diagram (Figure 1(a)) or by s-channel h production (Figure 1(b)), the latter of which features the trilinear h self coupling. In principle, this gives access to the self-coupling via measurements of the di-Higgs production rate at the LHC. Destructive interference between the two production processes, however, significantly reduces the cross section, making such measurements very challenging. On the other hand, physics beyond the SM could enhance the di-Higgs production rate, either through *resonant* production of a new particle, X (e.g. s-channel production of Kaluza-Klein gravitons), or through enhanced *non-resonant* production (e.g. existence of a direct *tthh* vertex).

In Run 1 of the LHC, ATLAS [1] developed a rich di-Higgs physics program, with searches in the *bbbb* ($\mathcal{B} = 34\%$), *bbττ* ($\mathcal{B} = 7\%$), *γγbb* ($\mathcal{B} = 0.26\%$) and *γγWW** ($\mathcal{B} = 0.1\%$) channels [2]. Updates of the searches in the *bbbb* [3], *γγbb* [4] and *γγWW** [5] channels using 3.2–13.3 fb^{-1} of integrated luminosity collected by the ATLAS detector in pp collisions at $\sqrt{s} = 13$ TeV produced by the LHC are presented in this report.
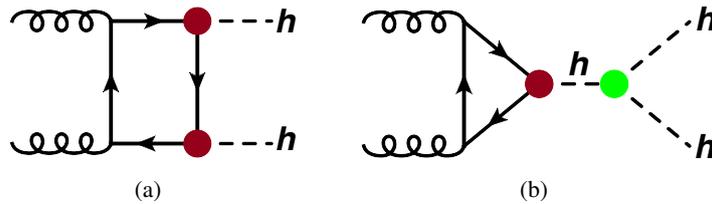
Figure 1: Standard Model di-Higgs production via (a) a box-diagram or (b) s-channel h production [4].

2. Search in the *bbbb* channel

Searches for low-mass resonant ($m_X \leq 1$ TeV) and non-resonant di-Higgs production in the *bbbb* channel are performed using a *resolved* analysis. To maintain high signal efficiency, the events are selected by a set of triggers requiring either one or two b-tagged jets with various kinematic and tagging criteria and in some cases additional jets. The events must contain at least four b-tagged jets with $p_T > 30$ GeV. Higgs boson candidates are formed by pairing jets with angular separation consistent with the signal. Further selection is placed on the p_T, angular separation and mass of the Higgs boson candidates. The total selection efficiency is 1–6%, which decreases at high resonance masses as the jets become too close to be resolved. For high-mass resonant production, a *boosted* analysis is performed. Events are selected by a single fat-jet ($R = 1.0$) trigger and must contain a leading (sub-leading) p_T fat-jet with $p_T > 450 (250)$ GeV. The fat-jets are trimmed to minimise impact from pileup and each one must have at least one associated b-tagged track jet ($R = 0.2$). The two fat jets must pass further selection on their angular separation and mass.

The dominant background contribution is from multijet production. It is estimated in the resolved (boosted) analysis by weighting events in a control region that contain exactly 2 (0) b-tagged jets by transfer factors calculated in a two dimensional side-band formed by the reconstructed masses of the Higgs boson candidates. In addition to normalising the sample, the transfer
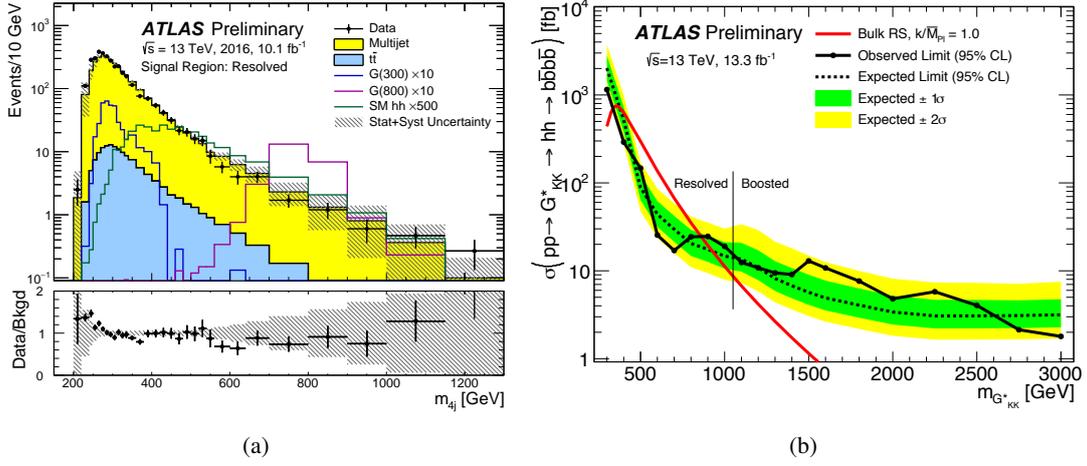
Figure 2: (a) Distribution of m_{4j} in the resolved signal region of the *bbbb* channel and (b) the expected and observed upper limit for $pp \to G^*_{KK} \to hh \to bbbb$ for a Kaluza-Klein graviton [3].

factors also include a kinematic reweight to account for kinematic biases from the *b*-tagging algorithm. The minor contribution from $t\bar{t}$ is estimated using simulation. The dominant uncertainties on the background prediction are due to the modelling of the Multijet contribution, evaluated using modifications to the control regions, and on the $t\bar{t}$ contribution, due to modelling of the initial- and final-state radiation. Their combined effect is 5–24% on the total background normalisation depending on the signal region. The dominant uncertainty on the signal prediction arises from modelling of the *b*-tagging efficiency, and can be as large as 58%.

Resonant and non-resonant signals are searched for using an extended profile likelihood fit to the four-jet (two-jet) mass distributions of the resolved (boosted) analyses (see Figure 2(a)). An upper limit of $\sigma(pp \to hh \to b\bar{b}b\bar{b}) < 330$ fb on non-resonant production is found at 95% CL, which corresponds to $\sim$29 times the expectation from the SM. Figure 2(b) shows the 95% CL upper limits for a spin-2 graviton.

3. Search in the $\gamma\gamma bb$ and $\gamma\gamma WW^*$ channels

Events in the $\gamma\gamma bb$ and $\gamma\gamma WW^*(\to l\nu jj)$ channels are selected with a diphoton trigger. The $\gamma\gamma bb$ events should contain two isolated photons with an invariant mass of 105–160 GeV and two *b*-tagged jets with an invariant mass of 95–135 GeV. The non-resonant search is performed by an unbinned fit to the diphoton mass distribution. In the resonant search, the diphoton mass window is tightened to 122–128 GeV, the four-momentum of the $b\bar{b}$ system is scaled so that $m_{b\bar{b}} = 125$ GeV (improving the $m_{\gamma\gamma bb}$ resolution by $\sim$60%) and $m_{\gamma\gamma bb}$ is required to be within a window that contains 95% of the signal events. A counting experiment is then performed to search for the signal. The $\gamma\gamma WW^*(\to l\nu jj)$ events should contain two isolated photons with an invariant mass of 122–128 GeV, an isolated electron or muon and two jets that are not *b*-tagged. A counting experiment is used to search for both resonant and non-resonant signals.

The dominant backgrounds for both channels arise from continuum diphoton production, which is estimated via data-driven techniques. For the $\gamma\gamma WW^*(\to l\nu jj)$ channel, the continuum
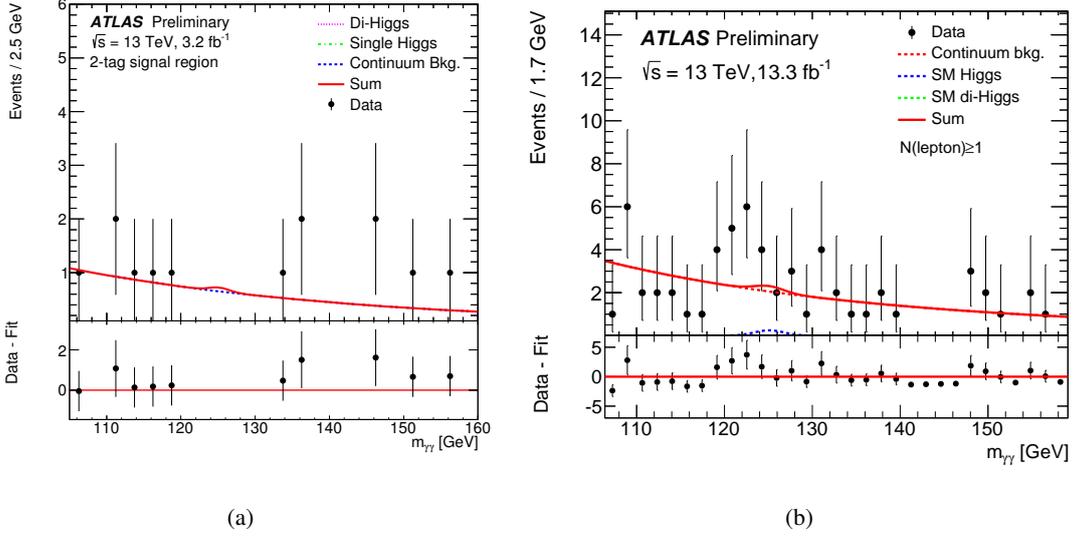
Figure 3: Diphoton mass distributions in the (a) $\gamma\gamma bb$ and (b) $\gamma\gamma WW^*$ channels [4, 5].

contribution is estimated by weighting events in a $m_{\gamma\gamma}$ sideband by a transfer factor that is calculated in a control region with the same selection as the signal region, but with no selected electrons or muons and a wider $m_{\gamma\gamma}$ window. For the resonant search in the $\gamma\gamma bb$ channel, a similar procedure is applied, with the following modifications. First, the transfer factor is calculated in a control region where both jets fail the *b*-tagging criteria (0-tag). Second, an additional transfer factor, calculated in the same region, is applied to account for the $m_{\gamma\gamma bb}$ selection. For the non-resonant search, the 0-tag region is included in the unbinned fit to help constrain the shape of the continuum background. In both channels, systematic uncertainties have little impact, as they are statistically limited.

The $m_{\gamma\gamma}$ distributions for the $\gamma\gamma bb$ and $\gamma\gamma WW^*(\to l\nu jj)$ channels are shown in Figures 3(a) and 3(b), respectively. Upper limits on non-resonant production of $\sigma(pp \to hh \to \gamma\gamma bb) < 10$ fb and $\sigma(pp \to hh \to \gamma\gamma WW^*) < 24$ fb are found at 95% CL, corresponding to $\sim$120 and $\sim$750 times the expectation from the SM, respectively. Figures 4(a) and 4(b) show the 95% CL upper limits for a heavy narrow resonance decaying to two light Higgs bosons in the $\gamma\gamma bb$ and $\gamma\gamma WW^*$ channels, respectively.

4. Future prospects

While the searches presented have not shown any sign of di-Higgs production, they only use a fraction of the available data collected by the ATLAS experiment. Furthermore, the high-luminosity LHC upgrade is expected to increase the current dataset size by roughly two orders of magnitude. Estimates of the achievable sensitivity in the *bbbb* and $\gamma\gamma bb$ channels have recently been performed [6, 7]. Figure 5 shows a projection of the expected 95% CL upper limit on $\sigma(pp \to hh \to b\bar{b}b\bar{b})$ as a function of the Higgs boson self coupling parameter under the assumption of negligible impact from systematic uncertainties. This study indicates a projected upper limit of $\sim$1.5 times the SM. Figure 5(b) compares cross section upper limits as a function of the integrated
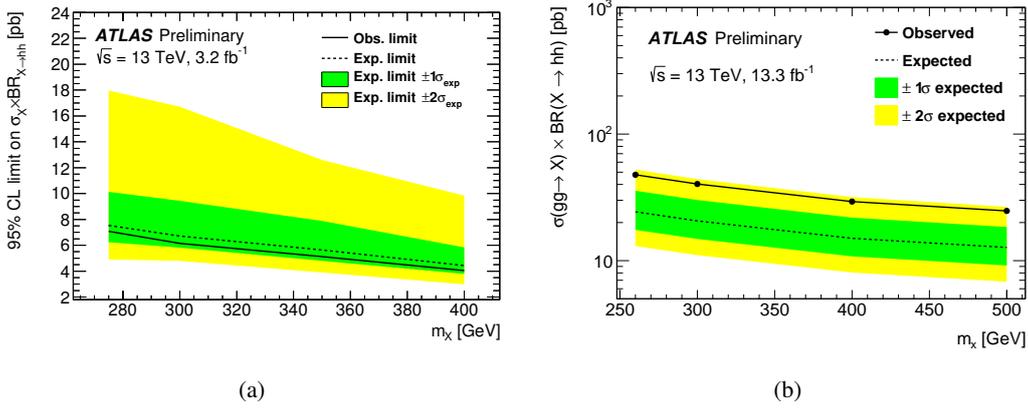
Figure 4: Upper limits at 95% CL on the production cross section times branching fraction for a heavy narrow resonance decaying to two light Higgs bosons in the (a) $\gamma\gamma bb$ and (b) $\gamma\gamma WW^*$ channels [4, 5].
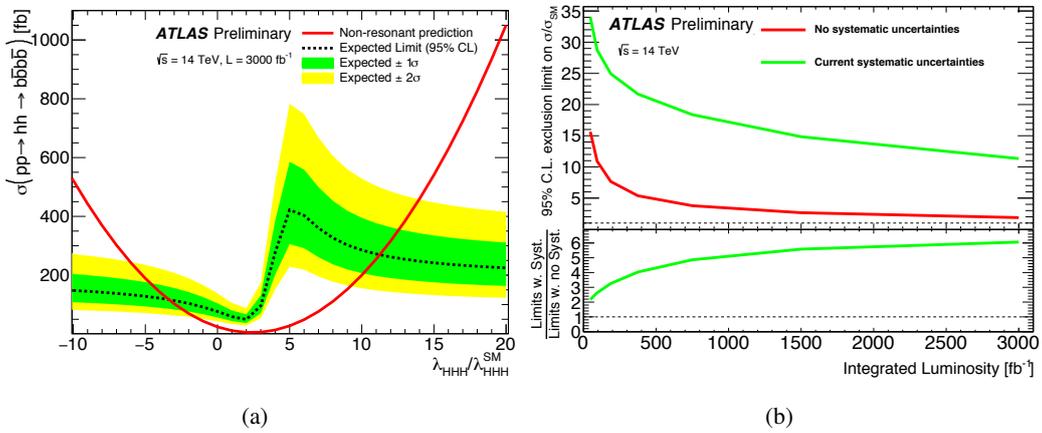
Figure 5: Projected 95% CL upper limits on di-Higgs production in the *bbbb* channel as a function of (a) the Higgs boson self coupling parameter and (b) the integrated luminosity [6].

luminosity in a scenario with no systematic uncertainties to a scenario including the current level of systematic uncertainties, highlighting the importance of reducing systematic uncertainties in the future. While the projected sensitivity of any individual channel alone is not enough to observe SM di-Higgs production, the *bbbb*, $\gamma\gamma bb$ and $bb\tau\tau$ channels each have similar projected sensitivities and the prospect of a combination is promising for an eventual observation at the LHC.

References

[1] ATLAS Collaboration, *The ATLAS Experiment at the CERN Large Hadron Collider*, JINST **3** (2008) S08003.

[2] ATLAS Collaboration, *Searches for Higgs boson pair production in the hh → bbττ, γγWW*, γγbb, bbbb channels with the ATLAS detector*, Phys. Rev. D **92**, 092004 (2015) [arXiv:1509.04670].

[3] ATLAS Collaboration, *Search for pair production of Higgs bosons in the b̄bb̄b final state using*

proton–proton collisions at $\sqrt{s} = 13\,TeV$ with the ATLAS detector, ATLAS-CONF-2016-049, https://cds.cern.ch/record/2206131.

[4] ATLAS Collaboration, *Search for Higgs boson pair production in the $b\bar{b}\gamma\gamma$ final state using pp collision data at $\sqrt{s} = 13\,TeV$ with the ATLAS detector*, ATLAS-CONF-2016-004, https://cds.cern.ch/record/2138949.

[5] ATLAS Collaboration, *Search for Higgs boson pair production in the final state of $\gamma\gamma WW^{*}(\rightarrow l\nu jj)$ using $13.3\,fb^{-1}$ of pp collision data recorded at $\sqrt{s} = 13\,TeV$ with the ATLAS detector*, ATLAS-CONF-2016-071, https://cds.cern.ch/record/2206222.

[6] ATLAS Collaboration, *Projected sensitivity to non-resonant Higgs boson pair production in the $b\bar{b}b\bar{b}$ final state using proton–proton collisions at HL-LHC with the ATLAS detector*, ATL-PHYS-PUB-2016-024, https://cds.cern.ch/record/2221658.

[7] ATLAS Collaboration, *Study of the double Higgs production channel $H(\rightarrow b\bar{b})H(\rightarrow \gamma\gamma)$ with the ATLAS experiment at the HL-LHC*, ATL-PHYS-PUB-2017-001, https://cds.cern.ch/record/2243387.